

tribute significantly to the stabilization of the complex. Alternatively, one can ignore rigorous assignment of formal oxidation states for the metal, and simply assume that the oxidation state is a property of the complex as a whole.

Finally, although less likely, is the possibility that the bridging superoxide may accept  $\pi$  electron density from the pyridyl ring, resulting in increased charge density at the nitrogen.

The similarity in spectra of the protonated ligand and metal ligand complex can be used to advantage in interpretation of d-d spectra. Normally, the strong  $\pi$ - $\pi^*$  bands of phenanthroline obscure d-d bands below 400 nm. However, using the protonated ligand in the reference cell allows one to obtain a "difference spectra" which is free of ligand bands above 350 nm. This technique was used to obtain the d-d spectra in Figure 2. The difference spectra as obtained by the method described could further be used to calculate ligand field parameters for the oxygenated complex. Normally, the high energy L  $\rightarrow$  M charge transfer band ( $\lambda_{\max} \sim 350$  for dioxygen complexes of cobalt aliphatic polyamines) obscures all spectral details below 400 nm in the peroxo complexes, making band assignments quite tenuous.

For the condensed pyridyl ligands, however, the charge transfer band is shifted to  $\sim 390$  nm, consistent with the poorer  $\sigma$  donor properties of the pyridyl nitrogens. (For a L  $\rightarrow$  M charge transfer, the energy should increase as the ligands donate more  $\sigma$  electron density to the metal, thus increasing the energy required for the transfer of charge to occur.) This shift, coupled with the difference spectra technique, enables resolution of the tetragonal component at  $\sim 367$  nm in the [Co(phen)<sub>2</sub>]<sub>2</sub>O<sub>2</sub>OH complex. Thus the energy of the <sup>1</sup>A  $\rightarrow$  <sup>1</sup>T transition can be approximately assigned as the arithmetic average of the tetragonal components (462, 367 nm), and  $\Delta E_{1A \rightarrow 1T} \approx 24\,040$  cm<sup>-1</sup>.

Using the equations of Lever<sup>12</sup>  $\Delta E = 100g + C - 80B^2/$

$10Dq$ . Without another band, which cannot be effectively resolved in this system,  $B$  cannot be obtained. However, for such a high field  $Dq/B > 4$ , and, taking  $C = 4B$ ,<sup>12</sup>  $\Delta E \approx 10Dq$ . Thus  $10Dq \approx 2040$  cm<sup>-1</sup> = [ $2Dq(\text{phen}) + Dq(\text{OH}) + Dq(\text{O}_2^{2-})$ ]. Using the tabulated values of Figgis<sup>13</sup> for phen ( $Dq = 8930$  cm<sup>-1</sup>) and OH<sup>-</sup> (2976 cm<sup>-1</sup>),  $Dq\text{O}_2^{2-} \approx 3200$  cm<sup>-1</sup>. Thus the ligand field strength of " $\mu$ -peroxo" dioxygen is slightly higher than that of H<sub>2</sub>O. This result is close to that obtained by Gray and Treitel<sup>14</sup> for (Co(NH<sub>3</sub>)<sub>5</sub>)<sub>2</sub>O<sub>2</sub> thus supporting their result, and is fully consistent with the chemistry of peroxide, which is a fairly weak  $\sigma$ -donor, and cannot act as a  $\pi$ -acceptor, as its  $\pi^*$  orbitals are filled.

**Acknowledgment.** The authors thank Dr. H. B. Gray for supplying prepublication information.

## References and Notes

- (1) (a) This work was supported by a research grant, No. GP-43752, from the National Science Foundation. (b) Texas A&M University Health Fellow. (c) Professor of Chemistry, University of Hartford, Hartford, Conn.; Visiting Professor of Chemistry, Texas A&M University, 1974-1975.
- (2) For recent reviews see R. G. Wilkins *Adv. Chem. Ser.*, No. 100, 111 (1971); A. G. Sykes and J. A. Weil, *Prog. Inorg. Chem.*, **13**, 1 (1970); and G. McLendon and A. E. Martell, *Coord. Chem. Rev.*, in press.
- (3) (a) G. McLendon, D. T. MacMillan, M. Hariharan, and A. E. Martell, *Inorg. Chem.*, **14**, 2322 (1975); (b) G. McLendon and A. E. Martell, *J. Chem. Soc., Chem. Commun.*, 223 (1975).
- (4) D. H. Huchital and A. E. Martell, *Inorg. Chem.*, **13**, 2966 (1974).
- (5) R. Nakon and A. E. Martell, *J. Am. Chem. Soc.*, **94**, 3026 (1972).
- (6) Y. Sasaki and K. Fujita, *Bull. Chem. Soc. Jpn.*, **42**, 2089 (1964).
- (7) K. M. Davies and A. G. Sykes, *J. Chem. Soc. A*, 1418 (1971).
- (8) J. Simplicio, Ph.D. Dissertation, State University of New York, Buffalo, 1969.
- (9) J. O. Gillard, *J. Chem. Soc. A*, 917 (1967).
- (10) C. J. Hawkins, "Absolute Configuration of Metal Complexes", Wiley-Interscience, New York, N.Y., 1971.
- (11) A. Werner and A. Mylius, *Z. Anorg. Chem.*, **16**, 245 (1898).
- (12) A. B. P. Lever, "Inorganic Electron Spectroscopy", Elsevier, New York, N.Y., 1968.
- (13) B. N. Figgis, "Introduction to Ligand Fields", Wiley-Interscience, New York, N.Y., 1969.
- (14) V. M. Miskowski, J. L. Robbins, I. M. Treitel, and H. G. Gray, *Inorg. Chem.*, in press.

## Infrared Spectral Studies of Metal Binding Effects on the Secondary Structure of Bean Plastocyanin

Jeffrey W. Hare, Edward I. Solomon, and Harry B. Gray\*

Contribution No. 5189 from the Arthur Amos Noyes Laboratory of Chemical Physics, California Institute of Technology, Pasadena, California 91125.

Received September 22, 1975

**Abstract:** The infrared spectra (4000-200 cm<sup>-1</sup>) of holo-, apo-, cobalt(II)-substituted, and heat- and acid-denatured bean plastocyanins (*Phaseolus vulgaris*) are assigned. Bands at 1260 and 370 cm<sup>-1</sup> in apoplastocyanin are shown to be dependent upon secondary conformation and are assigned to an  $\alpha$ -helix structure by comparison to homopolypeptide vibrational spectra and analysis of the ultraviolet circular dichroism spectrum of the holoprotein. Further, shifts upon metal incorporation to  $\sim 1245$  and  $345$  cm<sup>-1</sup>, respectively, suggest a metal-associated distortion of the helix to a more extended form. The ir data confirm that cobalt(II) substitutes at the copper site in bean plastocyanin. Based on all available vibrational spectral results, it is proposed that the metal ion is bound to a peptide linkage, which itself is part of a short section of helix present in the protein. There is no effect on this helical section of the site upon reduction of the holoprotein to its copper(I) form.

Recent x-ray photoelectron spectral (XPS) studies have shown<sup>1</sup> that copper is bound to a sulfur atom in plastocyanin isolated from French bean leaves (*Phaseolus vulgaris*). It has also been observed<sup>2</sup> in Raman spectroscopic experiments on the spinach protein that certain amide vibrations are resonance-enhanced, possibly as a result of association of copper with a side chain or a peptide linkage of the plastocyanin backbone. With the goal of learning more about the protein

environment in the vicinity of the metal site, we have made a detailed study of the infrared spectra of bean plastocyanin and several of its derivatives.

## Experimental Section

Solutions of holo-, reduced, apo-, and cobalt(II)-substituted bean plastocyanins were prepared as described previously.<sup>3</sup> The buffer was removed from the solutions by anaerobic dialysis at 4° against triply

**Table I.** Correlation of Polypeptide Vibrational Spectral Bands to Secondary Structure

Conformation	Mode <sup>a</sup>					
	Amide I	Amide II	Amide III	Amide IV	Amide V	Amide VI
$\alpha$ -Helix (ir)	1653-1659	1545-1550	1242-1276 1290-1298	524-541	609-625	654-668
(R)	1647-1654	1537-1549	1261-1300	662	756	610
Polyglycine II (ir)	1654	1554	1249, 1283	698	740	573
(Trigonal helix) (R)	1654		1244, 1283	673	742, 752	566
$\beta$ (ir)	1621-1636	-1548	1214-1224	529-564	695-708	612-617, 622-652
(R)	1685-1699		1235-1241			601
$\gamma$ (ir)	1668-1674	1531-1564	1231-1235		708	
(R)	1655	1535	1250		650	
(R)	1649-1683	1521-1565	1245-1261			

<sup>a</sup> Energies  $\text{cm}^{-1}$ .

distilled water which had been treated with Chelex resin to remove any trace metal ions. The solutions were then lyophilized by quick freezing in liquid nitrogen and evacuating to  $10^{-6}$  Torr. Plastocyanin was heat-denatured by dissolving lyophilized protein in triply distilled water, millipore filtering to remove any undissolved protein, and heating at  $75^\circ$  over a steam bath for 1 h. The heat-denatured sample was also quick frozen in liquid nitrogen and lyophilized. Acid denaturation was accomplished by dissolving 5 mg of plastocyanin in 1.5 ml of deoxygenated, triply distilled water. The solution was transferred to a specially designed pH cell, which was flushed with argon, and then concentrated hydrochloric acid was added until pH 2 was reached. After 30 min of stirring under argon at pH 2 in an ice bath, the solution was frozen and dried.

Samples for infrared spectral measurements were prepared by lightly grinding approximately 2.5 mg of lyophilized protein with the minimum amount of Vaseline needed to form a mull. The mull was spread on a freshly prepared cesium iodide pellet and covered with a second pellet. The sample was then cooled to 77 or 12 K in a Cryogenics Technology, Inc., Model 20 cryocooler equipped with cesium iodide windows and an adjustable temperature controller. Halocarbon grease mulls for the hydrocarbon ir regions were prepared in the same manner and spread between potassium bromide disks. All operations were performed in an argon- or nitrogen-filled glove bag to prevent protein oxidation and to minimize water and carbon dioxide absorption by the pellet material.

A thin film of plastocyanin was prepared by slow evaporation of a drop of concentrated, unbuffered protein solution on a silver bromide disk in a controlled-humidity desiccator at  $4^\circ$ . After the film had formed, a silicone rubber gasket and a second silver bromide disk were placed over it. This "sandwich" was then placed in the cryocooler for comparative spectral measurements.

Infrared spectra were measured using a Perkin-Elmer 180 grating spectrophotometer equipped with the far-infrared option. A manual slit mode set for 2-4  $\text{cm}^{-1}$  resolution above 500  $\text{cm}^{-1}$  and 4-6.5  $\text{cm}^{-1}$  resolution below 500  $\text{cm}^{-1}$  was routinely used.

A 0.096 mM solution of bean plastocyanin in 0.05 M acetate buffer at pH 6 was millipore filtered and placed in a 1-mm path length quartz cell. The CD spectrum of this solution was measured from 300 to 210 nm using a Cary 61 spectropolarimeter (resolution, 1 nm; sensitivity;  $0.1^\circ$  full scale).

## Results and Discussion

The predominant features of the vibrational spectra of polypeptides are in general attributable to motions of the basic structural unit, the amide linkage  $\text{C}_\alpha\text{-CONH-C}_\alpha'$ . The atomic motions may be designated as follows:<sup>4</sup> amide A ( $\nu_{\text{NH}}$ ), amide B ( $2 \times \delta_{\text{NH}}$  in Fermi resonance with  $\nu_{\text{NH}}$ ), amide I ( $\nu_{\text{CO}}$ ), amide II ( $\delta_{\text{NH}} + \nu_{\text{CN}}$ ), amide III ( $\nu_{\text{CN}} + \delta_{\text{NH}} + \nu_{\text{CC}_\alpha}$ ), amide IV ( $\delta_{\text{OCN}} + \nu_{\text{CC}_\alpha}$ ), amide V ( $\rho_{\text{NH}}$ ), amide VI ( $\rho_{\text{CO}}$ ), and amide VII ( $\tau$ ) ( $\nu$  represents a stretching motion,  $\delta$  in-plane bending,  $\rho$  out-of-plane bending, and  $\tau$  the torsional motion of the CONH plane). A summary of amide vibrational energy ranges as correlated<sup>5-12</sup> to polypeptide conformation is given in Table I. Attempts to extend these correlations to fibrous proteins have been reasonably successful. In globular proteins, however, only

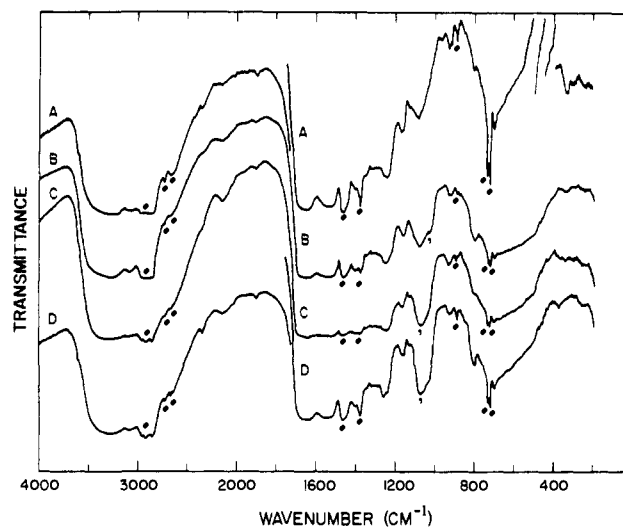


**Figure 1.** Vaseline mull infrared spectra of holo- (A), reduced (B), cobalt(II)-substituted (C), and apo- (D) plastocyanins. Peaks marked # are due to the mulling agent and peaks marked † are attributable to traces of buffer.

the Raman amide III band has shown adequate structure to make assignments that correspond to particular conformations.<sup>13-18</sup>

In the energy region below 400  $\text{cm}^{-1}$  in homo- and copoly-peptide spectra, Itoh and co-workers have assigned ir bands attributable to  $\alpha$ -helix and  $\beta$  sheet structures at 376-369 and 265-235  $\text{cm}^{-1}$ , respectively.<sup>7,9,10</sup> As the vibrations in question are admixtures of backbone angle deformations and the amide bond torsional mode allowed by specific coupling in an  $\alpha$  helix or  $\beta$  sheet, they are found at much lower energies in monomeric amino acids or in random coil structures.<sup>19,20</sup> Thus, they represent unique frequencies for determining secondary structure in proteins, as has been confirmed in studies<sup>21</sup> of myoglobin and collagen.

The Vaseline mull infrared spectra (4000-200  $\text{cm}^{-1}$ ) of holo- (A), reduced (B), cobalt(II)-substituted (C), apo- (D), heat-denatured (E), and acid-denatured (F) bean plastocyanins, as well as thin film (G) and halocarbon mull (H) spectra of the holoprotein, are presented in Figures 1 and 2. The amide I and II bands at 1650 and 1540  $\text{cm}^{-1}$ , respectively, are broadened over most of the range observed in polypeptide spectra. The amide IV-VI region from 750 to 450  $\text{cm}^{-1}$  is also broad, with structure appearing at 700  $\text{cm}^{-1}$  and a shoulder at 490  $\text{cm}^{-1}$ . The amide III region (1300-1230  $\text{cm}^{-1}$ ), however, shows distinct spectral features that are sensitive to protein modification at 1260 and 1240  $\text{cm}^{-1}$ .

The low energy region (525-200  $\text{cm}^{-1}$ ) of the ir spectra of

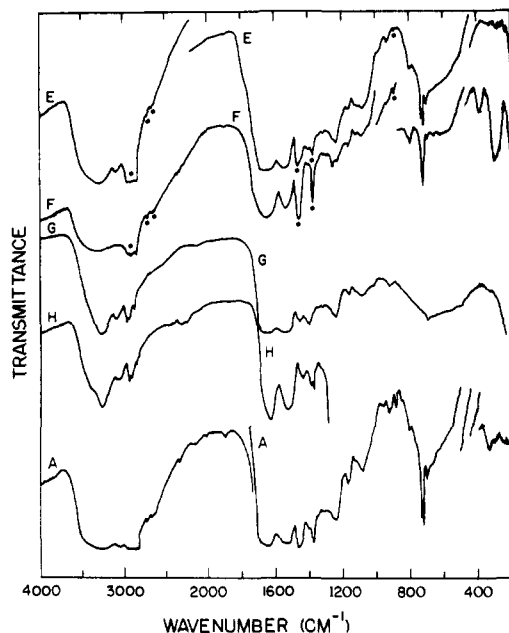


**Figure 2.** Vaseline mull infrared spectra of holo- (A), heat-denatured (E), and acid-denatured (F) plastocyanins, as well as thin film (G) and halocarbon mull (H) spectra of holoplastocyanin. Peaks marked # are due to the mulling agent.

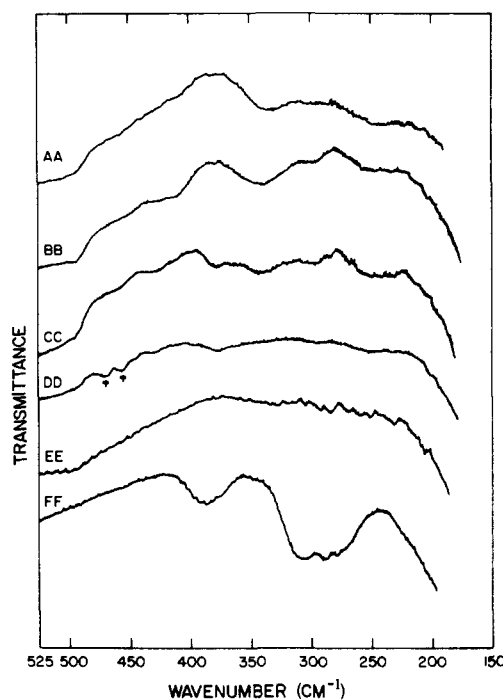


**Figure 3.** Expanded low energy infrared spectra of holo- (AA), reduced (BB), cobalt(II)-substituted (CC), apo- (DD), heat-denatured (EE), and acid-denatured (FF) plastocyanins.

Vaseline mulls of holo- (AA), reduced (BB), cobalt(II)-substituted (CC), apo- (DD), and heat-denatured (EE) samples of bean plastocyanin is expanded in Figure 3. Each of the metal-bound proteins exhibits an absorption band at  $345\text{ cm}^{-1}$  (AA, BB, and CC), which shifts to  $370\text{ cm}^{-1}$  (DD) when the metal is removed. Very little ( $\leq 10\%$ ) intensity at  $345\text{ cm}^{-1}$  remains in apoplastocyanin. There is no peak at either  $370$  or  $345\text{ cm}^{-1}$  or any other frequency in this region of the spectrum in the denatured sample (EE), although all other features are virtually identical with those in the metal-incorporated and apo-protein spectra. We conclude that the  $370\text{-cm}^{-1}$  band de-

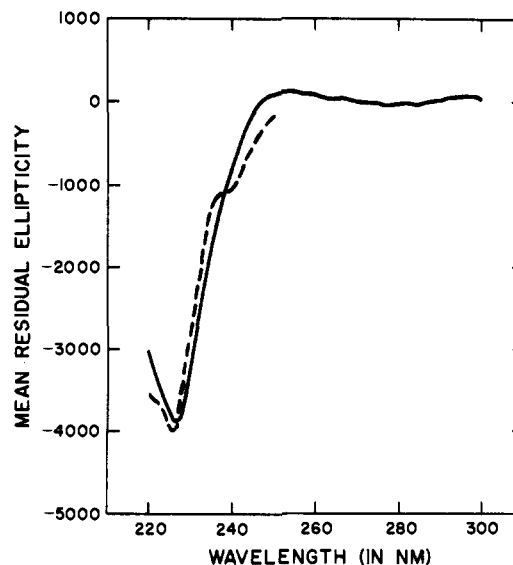


**Figure 4.** The natural circular dichroism spectrum of holoplastocyanin ( $0.096\text{ mM}$  in  $0.05\text{ M}$  acetate buffer,  $\text{pH } 6$ ,  $25^\circ$ ). The dashed line corresponds to the best fit spectrum calculated over the region  $220\text{--}250\text{ nm}$ .

pends on protein conformation and, further, is perturbed by the presence of the metal. Acidification to  $\text{pH } 2$  completely destroys the blue color of holoplastocyanin, indicating a large structural change in the protein. The infrared spectrum FF is sensitive to this change, as the low energy band shifts to  $380\text{ cm}^{-1}$  and is enhanced in intensity.

The  $370\text{-cm}^{-1}$  band in apoplastocyanin matches the energy of the backbone deformation in polypeptides containing  $\alpha$ -helices.<sup>7,9,10</sup> The shift observed upon metal incorporation probably is not a consequence of coordination of an appropriate side chain, as the only potential ligands that also absorb at  $370\text{ cm}^{-1}$  are aspartate and serine.<sup>22</sup> As there are five aspartate and eight serine residues in the primary sequence,<sup>23</sup> it seems extremely unlikely that only one of these units is vibrationally active. Complete absence of the low energy feature in the heat-denatured sample is also inconsistent with such an assignment.

As no intensity remains at  $370\text{ cm}^{-1}$  when copper is bound to plastocyanin, the entire helix structure in the protein must be perturbed. This result suggests that one relatively short helix (no more than about three turns) is present in the protein. Additional evidence in support of this suggestion was obtained from the ultraviolet CD spectrum of holoplastocyanin (Figure 4). The CD curve was least-squares fit to the set of standard spectra calculated by Chen et al.,<sup>24</sup> to determine relative amounts of the three principal conformations present. The best fit yielded 3% helix, 5% sheet, and 92% random coil. It should be noted that the percentage of helix is likely to be underestimated by this procedure, as the mean residual ellipticity has been shown to become less negative with decreasing helical length.<sup>24</sup>

A band at  $250\text{ cm}^{-1}$  appears in all the spectra of Figure 3 except DD, the heat-denatured sample. It appears that protein conformation is also reflected by this absorption. There are two modes in this energy region owing to backbone deformations, the torsional motion along the chains of the  $\beta$  sheet<sup>7</sup> and the symmetric breathing deformation of the  $\alpha$ -helix.<sup>11,25</sup> The mean value of reported frequencies in polypeptides containing the sheet conformation is  $249.6\text{ cm}^{-1}$ , with a standard deviation of  $10\text{ cm}^{-1}$ . The mean width at half maximum is  $38\text{ cm}^{-1}$ , with a deviation of  $13\text{ cm}^{-1}$ . The width at half maximum for the observed protein band is  $25\text{--}30\text{ cm}^{-1}$ , which accords quite well with the results from polypeptide spectra. Further, the band does not shift when metal is removed. The symmetric helix

deformation should shift to higher energy upon metal incorporation, as is found in comparing the  $\alpha$  to the trigonal helix in polypeptides. The lack of any shift establishes that  $\beta$ -sheet is also present in bean plastocyanin.

The amide III energy region is dominated by a band at 1240  $\text{cm}^{-1}$ . The intensity of this peak remains constant in all spectra except that of the acidified sample. In view of its position (see Table I) and the observation that no shift occurs upon removal of metal, the band is assigned to the amide III vibration of the composite sheet and random coil conformers present in plastocyanin. A shoulder at 1260  $\text{cm}^{-1}$  gains intensity in apoplastocyanin (D, Figure 1) and is even more prominent in the acid-denatured sample (F, Figure 2). This pattern is similar to that observed for the 370- $\text{cm}^{-1}$   $\alpha$ -helix deformation. Further, the shoulder is located in the energy region associated with the amide III motion of an  $\alpha$ -helix.<sup>11</sup> Therefore, the 1260- $\text{cm}^{-1}$  band is assigned to the  $\alpha$ -helix conformation present in apoplastocyanin. The corresponding amide III mode of the trigonal helix is observed at 1249  $\text{cm}^{-1}$  in polyglycine II.<sup>19</sup> This feature, which is expected to be present in metal-bound samples, is apparently masked by the strong 1240- $\text{cm}^{-1}$  peak. A weaker shoulder at 1260  $\text{cm}^{-1}$ , which occurs in all other samples, including heat-denatured plastocyanin, is attributable to a side chain vibration.

The infrared spectrum of cobalt(II) plastocyanin is identical with that of the holoprotein, except for an additional shoulder at 370  $\text{cm}^{-1}$ . This energy corresponds to the previously assigned helix mode of apoplastocyanin. The spectral data, therefore, are consistent with our earlier observation that incorporation of Co(II) into apoplastocyanin is about 70% effective.<sup>3</sup> Furthermore, the results show that the Co(II) that is incorporated distorts the  $\alpha$ -helix in the same manner as does the copper. Thus, both ir and XPS<sup>1</sup> experiments establish conclusively that Co(II) and Cu(II) bind at the same site in bean plastocyanin.

The presence of bands at 370 and 1260  $\text{cm}^{-1}$  in spectrum D (Figure 1) has been attributed to a section of  $\alpha$ -helix in the apoplastocyanin secondary structure. A shift from 370 to 345  $\text{cm}^{-1}$  and a decrease in intensity of the 1260- $\text{cm}^{-1}$  band are observed upon metal incorporation. These spectral changes may be interpreted in terms of a metal-induced distortion of the  $\alpha$ -helix to a form similar to polyglycine II.<sup>6,10</sup> It is unlikely, however, that a section of the polyglycine helix is present in the protein, because the stabilizing factor for this structure is intercoil hydrogen bonding.<sup>26</sup> However, the trigonal coil of a  $3_{10}$  helix, which does contain the necessary intracoil hydrogen bonding for a stable protein conformation, is expected to have a similar energy for the deformation mode. This mode is made up mainly of backbone angle deformations and the amide torsional motion. If hydrogen bonding were to affect this mode, the deuterated polyglycine spectrum should show a considerable shift in the 363- $\text{cm}^{-1}$  band. As the isotopic shift has been measured to be only 7  $\text{cm}^{-1}$ ,<sup>6</sup> the amide deformation of polyglycine II should be comparable in energy to the corresponding mode in the  $3_{10}$  helix.

Resonance Raman spectral studies of several blue proteins, including spinach plastocyanin, have shown enhancement of amide modes at 750, 1240, and 1650  $\text{cm}^{-1}$ , indicating an amide oxygen or nitrogen is coordinated to the copper.<sup>2</sup> In model complexes containing primary amide ligands, the carbonyl stretch occurs between 1680 and 1690  $\text{cm}^{-1}$ , and does not shift upon coordination either to nitrogen or oxygen.<sup>27</sup> As both asparagine and glutamine also have side chain carbonyl bands around 1680  $\text{cm}^{-1}$ ,<sup>28</sup> which are not expected to shift appreciably upon metal coordination, the amide side chains can be ruled out as possible ligands in plastocyanin. Further, the observed frequencies correspond quite well to A symmetry amide V, III, and I modes, respectively, in polyglycine II.<sup>19</sup> The 345- $\text{cm}^{-1}$  band is not resonance-enhanced, but this is a prob-

able result of the fact that the mode has E symmetry in the helix. As A symmetry modes are usually more intense in Raman spectra than E ones, the results are consistent with copper being bound to the backbone of a helix. It is of interest that the same bands are weakly enhanced in all blue copper proteins that have been studied, with no more than a 10- $\text{cm}^{-1}$  variation in each of the frequencies.<sup>2</sup> Thus, each of the entire group of blue proteins would appear to have a copper(II) bound to the amide backbone of a short section of a trigonal or distorted  $\alpha$ -helix.

It should be emphasized that we cannot distinguish between a metal-perturbed  $\alpha$ -helix and a rearrangement to a  $3_{10}$  type of structure. The major difference between the two helical structures is the position of the amide hydrogen-carbonyl oxygen hydrogen bond. This bond occurs between every four residues in the  $\alpha$ -helix, whereas it appears once in three in the  $3_{10}$  structure, thereby forcing it into a tighter coil with a greater pitch between turns. Coordination of copper to an amide nitrogen or oxygen associated with the helix could result in the loss of a hydrogen bond and destabilization of the structure. By breaking an  $\alpha$ -helix hydrogen bond, and shifting to the  $3_{10}$  structure, net loss of hydrogen bonds does not occur. Thus the structure is stabilized at the expense of higher coil strain energy. A similar mechanism has been proposed by Heitz et al. to explain the heat-induced transformation of poly- $\gamma$ -benzyl DL-glutamate from an  $\alpha$ -helix to the  $\pi$  (4.4<sub>16</sub>) structure.<sup>29</sup>

In summary, we have found helical secondary structure to be associated with the metal site in bean plastocyanin. It is likely that such structure also is present in other blue copper proteins. The short section of helix is distorted by metal (copper or cobalt) incorporation, which is probably the result of coordination to an amide nitrogen or oxygen of the peptide backbone. Finally, the perturbed helical structure at the site remains conformationally rigid upon reduction of holoplastocyanin to the copper(I) derivative.

**Acknowledgments.** We thank Professors P. J. Stephens and G. R. Rossman for allowing us to use instruments in their laboratories. One of us (E.I.S.) acknowledges the National Institutes of Health for a postdoctoral research fellowship. This research was supported by the National Science Foundation.

## References and Notes

- (1) E. I. Solomon, P. J. Clendening, H. B. Gray, and F. J. Grunthaner, *J. Am. Chem. Soc.*, **97**, 3878 (1975).
- (2) O. Silman, N. M. Young, and P. R. Carey, *J. Am. Chem. Soc.*, **96**, 5583 (1974); *ibid.*, **98**, 744 (1976).
- (3) D. R. McMillin, R. C. Rosenberg, and H. B. Gray, *Proc. Natl. Acad. Sci. U.S.A.*, **71**, 4760 (1974).
- (4) T. Miyazawa, T. Shimanouchi, and S.-I. Mizushima, *J. Chem. Phys.*, **29**, 611 (1958).
- (5) T. Miyazawa in "Polyamino Acids, Polypeptides, and Proteins", M. A. Stahmann, Ed., University of Wisconsin Press, Madison, Wisc., 1962.
- (6) S. Suzuki, Y. Iwashita, T. Shimanouchi, and M. Tsuboi, *Biopolymers*, **4**, 337 (1966).
- (7) K. Itoh, T. Shimanouchi, and M. Oya, *Biopolymers*, **7**, 649 (1969).
- (8) Y. Masuda, K. Fukushima, T. Fujii, and T. Miyazawa, *Biopolymers*, **8**, 91 (1969).
- (9) K. Itoh and H. Katabuchi, *Biopolymers*, **11**, 1593 (1972).
- (10) K. Itoh and H. Katabuchi, *Biopolymers*, **12**, 921 (1973).
- (11) J. L. Koenig and P. L. Sutton, *Biopolymers*, **10**, 89 (1971).
- (12) M. C. Chen and R. C. Lord, *J. Am. Chem. Soc.*, **96**, 4750 (1974).
- (13) R. C. Lord and N.-T. Yu, *J. Mol. Biol.*, **50**, 509 (1970).
- (14) R. C. Lord and N.-T. Yu, *J. Mol. Biol.*, **51**, 203 (1970).
- (15) J. L. Koenig and B. G. Frushour, *Biopolymers*, **11**, 2505 (1972).
- (16) N.-T. Yu and B. H. Jo, *Arch. Biochem. Biophys.*, **156**, 469 (1973).
- (17) B. G. Frushour and J. L. Koenig, *Biopolymers*, **14**, 379 (1975).
- (18) B. G. Frushour and J. L. Koenig, *Biopolymers*, **14**, 649 (1975).
- (19) E. W. Small, B. Fanconi, and W. L. Peticolas, *J. Chem. Phys.*, **52**, 4369 (1970).
- (20) B. Fanconi, E. W. Small, and W. L. Peticolas, *Biopolymers*, **10**, 1277 (1971).
- (21) (a) Yu. N. Cirkadze and A. M. Ovsepyan, *Biopolymers*, **12**, 637 (1973); (b) P. L. Gordon, C. Huang, R. C. Lord, and I. V. Yanniss, *Macromolecules*, **7**, 955 (1974).
- (22) F. F. Bentley, L. D. Smithson, and A. L. Rogak, "Infrared Spectra and Characteristic Frequencies  $\sim 700$ - $300$   $\text{cm}^{-1}$ ", Interscience, New York, N.Y., 1968.
- (23) P. R. Milne, J. R. E. Wells, and R. P. Ambler, *Biochem. J.*, **143**, 691 (1974).

- (24) Y.-H. Chen, J. T. Yang, and H. M. Martinez, *Biochemistry*, **11**, 4120 (1972).  
 (25) K. Itoh and T. Shimanouchi, *Biopolymers*, **9**, 383 (1970).  
 (26) F. H. C. Crick and A. Rich, *Nature (London)*, **176**, 780 (1955).  
 (27) A. W. McLellan and G. A. Melson, *J. Chem. Soc. A*, 137 (1967).

- (28) L. Simons, G. Bertstrom, G. Blomfelt, S. Forss, H. Stenback, and G. Wansen, *Comments Phys. Math., Soc. Sci., Fenn., Helsinki-Helsingfors*, **42**, 125 (1972).  
 (29) F. Heitz, B. Lotz, and G. Spach, *J. Mol. Biol.*, **92**, 1 (1975).

## Structural and Electronic Spectroscopic Investigation of $[(\text{Me}_2\text{N})_3\text{C}_3]_2[\text{Pt}_2\text{Cl}_6]$

Charles D. Cowman, Jack C. Thibeault, Ronald F. Ziolo, and Harry B. Gray\*

Contribution No. 5097 from the Arthur Amos Noyes Laboratory of Chemical Physics, California Institute of Technology, Pasadena, California 91125.

Received April 25, 1975

**Abstract:** The crystal structure of  $[(\text{Me}_2\text{N})_3\text{C}_3]_2[\text{Pt}_2\text{Cl}_6]$  has been determined from three-dimensional x-ray data collected by counter techniques using Mo  $K\alpha$  monochromatized radiation. The structure was refined by full-matrix least-squares methods using 4451 nonzero reflections for which  $F^2 > \sigma(F^2)$ , and assuming anisotropic thermal motion for all nonhydrogen atoms. The least-squares refinement led to a final value of the conventional  $R$  factor (on  $F$ ) of 0.058. Crystal data are as follows: monoclinic, space group  $P2_1/c$ ;  $a = 17.383$  (11),  $b = 11.234$  (6),  $c = 17.192$  (11) Å;  $\beta = 117.46$  (5)° (23 °C);  $Z = 4$ ;  $d_{\text{obsd}} = 2.12$ ,  $d_{\text{calcd}} = 2.09$  g/cm<sup>3</sup>. Discrete  $\text{Pt}_2\text{Cl}_6^{2-}$  anions are sandwiched between two parallel cyclopropenium cations. These sandwiched units are in turn stacked to form zigzag chains parallel to the crystallographic  $b$  axis. The two crystallographically independent cyclopropenium cations do not differ significantly. Coordination about each platinum atom in  $\text{Pt}_2\text{Cl}_6^{2-}$  is planar to a good approximation, but there is a fold of 10 (1)° about the Cl(1)–Cl(2) axis. The Pt–Pt distance in the anion is 3.481 (2) Å. The polarized electronic absorption spectra of a single crystal of  $[(\text{Me}_2\text{N})_3\text{C}_3]_2[\text{Pt}_2\text{Cl}_6]$  have been measured at 5 K. The spectra have been resolved into absorption profiles along the molecular axes of  $\text{Pt}_2\text{Cl}_6^{2-}$ . Three prominent  $y$ -polarized bands are observed, at 19 650, 24 600, and 26 250 cm<sup>-1</sup>. The 19 650-cm<sup>-1</sup> band is assigned to the  $y$ -allowed transition  $^1A_g \rightarrow B_{2u}$  ( $^3A_u$ ), whereas the 24 600- and 26 250-cm<sup>-1</sup> features are attributed to  $^1A_g \rightarrow B_{2u}$  ( $^1B_{2u}$ ) excitations derived from  $^1A_{1g} \rightarrow ^1A_{2g}$  ( $d_{x^2-y^2} \rightarrow d_{xy}$ ) in  $D_{4h}$   $\text{PtCl}_4^{2-}$ . The intensity enhancement of the  $^1A_g \rightarrow B_{2u}$  ( $^3A_u$ ) transition and the 1650-cm<sup>-1</sup> splitting observed for the  $^1A_g \rightarrow B_{2u}$  ( $^1B_{2u}$ ) bands conclusively establish that moderate Pt...Pt interactions are present in  $\text{Pt}_2\text{Cl}_6^{2-}$ . Detailed examination of the  $\text{Pt}_2\text{Cl}_6^{2-}$  polarized spectra also shows that the lowest excited states in the  $[\text{Pt}^{\text{II}}\text{Cl}_4]$  chromophore increase energetically according to  $^3E_g < ^3A_{2g} < ^3B_{1g} < ^1A_{2g}$ .

There has been considerable recent interest in the electronic spectra of Pt(II) complexes in which direct metal–metal interactions are present.<sup>1</sup> Perhaps the best studied cases are the double salts, such as  $[\text{Pt}(\text{NH}_3)_4][\text{PtCl}_4]$  (Magnus' green salt), in which the planar units stack face-to-face in infinite columns.<sup>1</sup> Much less is known, however, about the extent of Pt...Pt interaction in planar, dihalobridged complexes of the type  $\text{Pt}_2\text{X}_6^{2-}$ . The polarized electronic absorption spectra of a single crystal of  $[\text{Et}_4\text{N}]_2[\text{Pt}_2\text{Br}_6]$  were interpreted by Day et al.<sup>2</sup> in terms of an effectively isolated  $[\text{Pt}^{\text{II}}\text{Br}_4]$  chromophore, although later work by Martin<sup>3</sup> on the same system has indicated that some Pt...Pt interaction is present.

We have chosen to probe the  $\text{Pt}_2\text{Cl}_6^{2-}$  complex for possible Pt...Pt interactions, as the electronic structure of the reference monomer,  $\text{PtCl}_4^{2-}$ , has been exhaustively investigated by theoretical and experimental methods.<sup>4</sup> Here we report full details of the x-ray structure analysis<sup>5</sup> and the 5 K polarized electronic absorption spectra of a single crystal of  $[(\text{Me}_2\text{N})_3\text{C}_3]_2[\text{Pt}_2\text{Cl}_6]$ .

### Experimental Section

**Collection and Reduction of X-Ray Intensity Data.** A well-formed crystal of  $[(\text{Me}_2\text{N})_3\text{C}_3]_2[\text{Pt}_2\text{Cl}_6]$ ,<sup>6</sup> shaped like an octahedron compressed along the  $C_3$  axis, was chosen for x-ray diffraction study. The crystal had eight well-developed faces and gave good optical extinction between crossed polarizers. It was mounted with the  $b$  axis (from extinction direction and dichroism) approximately parallel to the rotation axis. A series of Weissenberg and precession photographs taken with Mo  $K\alpha$  and Cu  $K\alpha$  radiations indicated systematic absences of reflections  $h0l$  with  $l$  odd and  $0k0$  with  $k$  odd. The crystals were assigned to the monoclinic system, space group  $P2_1/c$ . The measured density of the crystal, by  $\text{CCl}_4$  displacement, is 2.12 g/cm<sup>3</sup>.

The calculated density, assuming four formula units per unit cell, is 2.09 g/cm<sup>3</sup>.

Fourteen reflections ( $2\theta > 20^\circ$ ) were centered in the counter aperture by varying  $2\theta$ ,  $\phi$ , and  $\chi$  in conjunction with the left–right and top–bottom balancing features of the variable receiving aperture. The cell constants and their standard deviations were determined by a least-squares refinement of the  $2\theta$  values for these 14 reflections. The results (Mo  $K\alpha$  radiation,  $\lambda$  0.71069) are  $a = 17.383$  (11) Å,  $b = 11.234$  (6) Å,  $c = 17.192$  (11) Å, and  $\beta = 117.46$  (5)° (23 °C). The corresponding  $\phi$  and  $\chi$  values for 13 of the reflections were used as input data for the orientation program operating under the CRYM crystallographic computing system.<sup>7</sup> The independent intensity data set was collected at 23 °C from a single-crystal mounted with its  $b$  axis approximately parallel to the  $\phi$  axis of a Datex-automated General Electric diffractometer.

A total of 5248 independent reflections were collected by the  $\theta$ – $2\theta$  scan technique in the range  $4^\circ < 2\theta$  (Mo  $K\alpha$ )  $\leq 50^\circ$ . A takeoff angle of  $3^\circ$  was used with the counter wide open. A check of several high-angle reflections indicated that our settings included the entire peak in the scan. The pulse height analyzer was set for approximately a 90% window centered on the Mo  $K\alpha$  peak. Mo  $K\alpha$  monochromatized radiation, obtained by using a single graphite crystal, was used for data collection. A scan rate of  $1^\circ/\text{min}$  (in  $2\theta$ ) was used with stationary counter, stationary crystal background counts of 30 s duration taken at each end of the scan. A symmetric scan range of between 1.5 and  $2.0^\circ$  was adjusted to account for  $\alpha_1$ – $\alpha_2$  splitting.

Throughout the data collection the intensities of three reference reflections were measured every 60 reflections. There were no signs of crystal decomposition in the x-ray beam.

The values for the observed intensities,  $I_{\text{obsd}}$ , were derived from the scalar counts using the formula

$$I_{\text{obsd}} = S - \frac{B_1 + B_2}{2} \left( \frac{t}{30} \right)$$